This article has been accepted for publication in a future issue of this journal, but has not been fully edited. Content may change prior to final publication. Citation information: DOI 10.1109/TMI.2015.2487866, IEEE Transactions on Medical Imaging

Evaluation of the accuracy of liver lesion DCEUS quantification with respiratory gating

Damianos Christofides, *Student Member, IEEE*, Edward Leen, and Michalakis A. Averkiou, *Senior Member, IEEE*

***Abstract*— Confidence in the accuracy of dynamic contrast enhanced ultrasound (DCEUS) quantification parameters is imperative for the correct diagnosis of liver lesion perfusion characteristics. An important source of uncertainty in liver DCEUS acquisitions is artifacts introduced by respiratory motion. The objective of this study is to construct a respiratory motion simulation model (RMSM) of dual contrast imaging mode acquisitions of liver lesions in order to evaluate an algorithm for automatic respiratory gating (ARG). The respiratory kinetics as well as the perfusion models of the liver lesion and parenchyma used by the RMSM were solely derived from clinical data. The quality of fit (of the DCEUS data onto the bolus kinetics model) depends on the respiration amplitude. Similar trends in terms of quality of fit as a function of respiration amplitude were observed from RMSM and clinical data. The errors introduced on the DCEUS quantification under the influence of respiration were evaluated. The RMSM revealed that the error in the liver lesion DCEUS quantification parameters significantly decreased($p<0.001$) from a maximum of 32.3% to 6.2% when ARG was used. The use of RMSM clearly demonstrates the capability of the ARG algorithm in significantly reducing errors introduced from both in-plane and out-of-plane respiratory motion.**

***Index Terms*—Medical simulation, Ultrasonic imaging, Contrast agents, Liver metastases, Respiratory gating**

I. Introduction

In their more than fifteen years of use [1] microbubble contrast agents have been used in many clinical applications. These include the diagnosis of liver lesions [2], the assessment of microvascular damage after a myocardial infarction [3] and the detection of coronary disease [4]. Microbubbles are a pure blood pool contrast agent, because their size is of the same order as red blood cells and thus cannot leave the vascular bed and escape in the interstitium [5], [6]. Their size along with their unique acoustic properties allow for the imaging of perfusion in real time using diagnostic ultrasound.

Manuscript submitted September 6, 2015.

D. Christofides is with the Department of Mechanical and Manufacturing Engineering, University of Cyprus, Nicosia, Cyprus

E. Leen is with the Imaging Department of Hammersmith Hospital, London, U.K.

M. A. Averkiou is with the Department of Bioengineering, University of Washington, Seattle, WA 98195-5061 USA (e-mail: maverk@uw.edu).

Microbubbles can be used to perform dynamic contrast enhanced ultrasound (DCEUS) for the characterization of liver lesions[7]. Muhi et al[8] compared the sensitivity of DCEUS, contrast enhanced computed tomography (CECT) and contrast enhanced magnetic resonance imaging (CEMRI) in detecting metastatic liver lesions from patients with primary colorectal cancer. The sensitivity of DCEUS was found to be 73% which compared favorably with the 63% sensitivity of CECT although it was significantly lower than the 95% sensitivity exhibited by CEMRI. Tranquart et al[9] demonstrated a similar sensitivity of 79.4% for DCEUS in the characterization of 1034 liver lesions as malignant or benign. Furthermore DCEUS is a safe imaging modality since it does not make use of ionizing radiation like CECT and it can be used on patients with pacemakers and ferromagnetic metal implants unlike CEMRI. In addition to its safety and clinical efficiency liver lesion DCEUS is cost effective and it can provide savings of 19% and 52% compared with CECT and CEMRI respectively[9].

Studies have been published in the literature [10]–[12] that use microbubbles to quantify liver lesion perfusion for early evaluation of patient response to treatment. These studies use modeling of the tumor perfusion to extract quantification parameters in order to make the evaluation of the response to treatment more objective than visual assessment and provide an early detection of response [13], [14]. Ideally these quantification parameters would be affected only by the blood flow and volume which in turn are related to the concentration of the microbubbles in the lesion under investigation. This is almost impossible to achieve due to factors that can affect the signal intensity detected by the imaging system like nonlinear propagation of ultrasound [15], signal saturation [16], and stability of ultrasound probe placement.

Further to the DCEUS acquisition problems mentioned there is the problem of physiological motion which can also have a negative impact on the quantification of blood flow and volume. Respiratory motion has the potential to move and deform the anatomy being imaged in relation to the imaging plane being acquired. In quantitative DCEUS for liver lesions the clinician needs to delineate the tumor using a region-of-interest (ROI) in order to extract the signal from within the lesion. However due to respiratory motion, the lesion moves in and out of the ROI. Thus the DCEUS linear intensity signal extracted from within the ROI can also have a component derived from sampling of normal liver parenchyma and/or

This article has been accepted for publication in a future issue of this journal, but has not been fully edited. Content may change prior to final publication. Citation information: DOI 10.1109/TMI.2015.2487866, IEEE Transactions on Medical Imaging

vessels. Respiration can also obscure visual details in the qualitative assessment of liver lesion DCEUS such as the lesion's feeding vessels since different cross sections of the lesion appear on the imaging plane due to out-of-plane respiratory motion.

A clinically used approach to compensate for the effects of respiratory motion is to direct patients to perform breath-holds [17]. However this approach can only by applied to patients that are able to hold their breath for a substantial period of time. Further to the practical problems breath-holds can also affect hemodynamics [18].

Post-processing procedures can also be implemented to negate the effect of respiratory motion for DCEUS quantification of liver lesions. One technique proposed by Averkiou et al [10] is for the clinician to manually reject frames in which the diaphragm position deviates from a reference location. This technique does not require any special precautions to be taken during the DCEUS acquisition and although it is implemented after the acquisition it can be very time consuming since all the steps of the procedure are manual.

Automation of correcting for respiratory motion can also be achieved using computational methods [19]–[23]. Disadvantages of these methods include the need for user intervention [20], [21], [23], extraction of only the end-phases of the respiration cycle [19], [20], and speed of execution [23].

A fully automatic respiratory gating (ARG) algorithm has been presented in the literature that is capable of significantly increasing the reliability of DCEUS quantification[24], [25]. The ARG algorithm can typically process 1000 frames in 8 seconds and it can extract any breathing cycle phase required by the user. The only manual intervention needed by the ARG algorithm is that the user chooses a "trigger" frame thus selecting the image (tumor) plane to be analyzed. Even though the ARG algorithm has been shown to increase the quality of fit of the lognormal indicator dilution model[26] onto liver lesion time intensity curves[24] it is impossible to determine the absolute gain in accuracy since it is impossible to know the true lesion perfusion in-vivo. The solution to this obstacle is the use of a simulation of a liver DCEUS acquisition in which the perfusion of the lesion is calculated using an indicator dilution model.

The objective of this work is to evaluate the efficiency of the ARG algorithm[25] in increasing the absolute accuracy of liver lesion DCEUS quantification using the controlled environment of a respiratory motion simulation model (RMSM) of dual contrast imaging mode liver lesion acquisitions.

II. Materials And Methods

A. Respiratory Motion Simulation Model

The RMSM was constructed in order to simulate a dual contrast imaging mode acquisition of liver lesions. During clinical acquisitions of liver DCEUS both in-plane and out-of-plane respiratory motion can affect the lesion's shape, size, and location in the image. Furthermore the appearance of structures like the diaphragm is also influenced by respiratory motion and is easily observed on the tissue side of the acquisition (Fig. 1). These changes in the appearance of the lesion and bright structures (e.g. the diaphragm) induced by respiratory motion were incorporated into the RMSM.

The RMSM was constructed in MATLAB® (2012b, The MathWorks Inc., Natick, MA) by generating image loops of a spherical lesion imbedded in a liver-like structure in the presence of cyclic respiratory motion. A dual contrast imaging mode was simulated, where the left side displayed the contrast image and the left side the tissue. The brightness of the contrast enhanced signal of the lesion and liver was programmed according to lognormal indicator dilution models derived from mean values of quantification parameters extracted from clinical DCEUS acquisitions (see section II.B). Specifically the lognormal indicator dilution model was fitted onto the clinical lesion time intensity curves and the mean values of the extracted quantification parameters of RT, MTT and PI were calculated.

The lesion was perfused according to the lognormal model[26] with a rise time (RT) of 17 seconds, a mean transit time (MTT) of 80 seconds and a peak intensity (PI) of 17 AIU (arbitrary intensity units). The parenchyma was perfused with a RT of 30 seconds, a MTT of 62 seconds and a PI of 33 AIU (Fig. 2). On the tissue side of the acquisition constant intensity levels were kept between a low intensity background and a 50% higher intensity moving structure. The total simulation time was 74 seconds, the frame rate was set to 8Hz and the imaging plane consisted of 300 by 300 pixels (px).

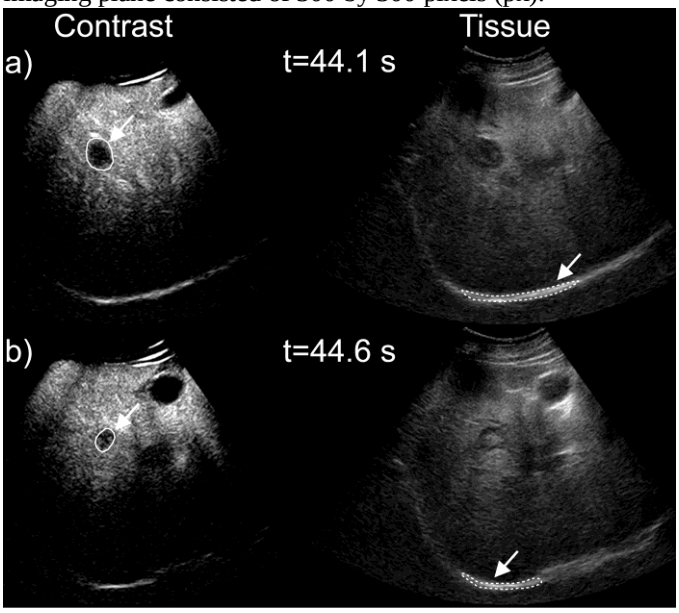

Fig. 1. Example of a clinical dual contrast imaging mode acquisition showing the contrast side (left) and the tissue side (right) at two time instances from the time of microbubble injection. At 44.1 s from the microbubble bolus injection a) the lesion (solid outline) can be clearly seen on the imaging plane whereas 0.5 s after b) the lesion appears altered in shape, size, and location. The diaphragm (dashed outline) has changed in position and dimensions due to both in-plane and out-of-plane motion.

The lesion was modeled as a sphere approximating the ellipsoid appearance of lesions seen in clinical acquisitions (Fig. 1). The radius of the lesion was set at 20px (R_L)

This article has been accepted for publication in a future issue of this journal, but has not been fully edited. Content may change prior to final publication. Citation information: DOI 10.1109/TMI.2015.2487866, IEEE Transactions on Medical Imaging

corresponding to the median liver lesion size from the clinical study and the parenchyma as a cube containing the lesion. In-plane and out-of-plane respiratory motion was produced by varying the position and radius of the lesion respectively according to a normalized respiratory kinetics curve (*G(t)*) that was extracted from patient data (Fig. 3). A set of liver lesion radii [*r(t)*] corresponding to each time instance in the acquisition were calculated using (1) and the values of the in-plane translation [*Δr(t)*] of the liver lesion were determined using (2),

$$r(t) = \sqrt{R_L{}^2 - \left(OPA \times G(t)\right)^2}\,, \tag{1}$$

$$\overrightarrow{\Delta r}(t) = IPA \times G(t)\left(\vec{i} + \vec{j}\right), \tag{2}$$

where *G(t)* was the patient derived normalized respiratory kinetics curve, R_L=20px, *t* was the time instance during the acquisition, *OPA* was a scalar defining the out-of-plane amplitude attributed to out-of-plane respiratory motion and *IPA* was a scalar defining the in-plane amplitude attributed to in-plane respiratory motion (Fig. 4a). On the tissue side of the acquisition the bright moving structure was modeled as a triangular prism captured as a rectangle on the imaging plane as a representation of the oblong appearance of the diaphragm in clinical studies (Fig. 1). The width of the rectangle was set to a constant value of 50 px and the values of the height of the triangle captured on the imaging plane were calculated using

$$h(t) = h_0 - \frac{OPA \times G(t)}{2}, \tag{3}$$

where *G(t)* was the patient derived normalized respiratory kinetics curve, h_o=20px, *t* was the time instance during the acquisition and *OPA* was a scalar specifying the out-of-plane amplitude attributed to out-of-plane respiratory motion (Fig. 4b). In plane motion was imposed by varying the center of the rectangle according to (2).

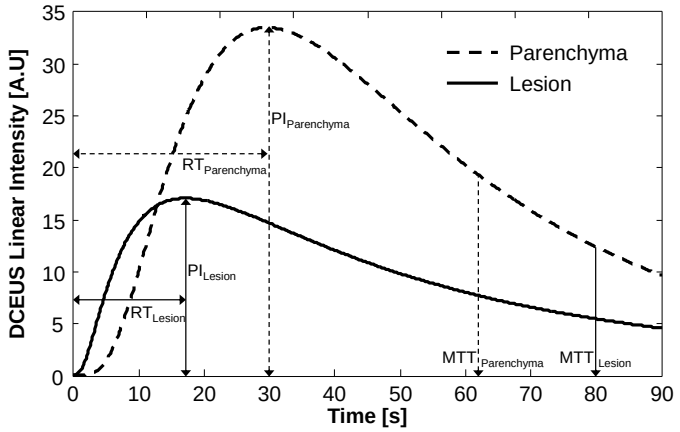

Fig. 2. Lognormal indicator dilution model time intensity curves used to calculate the linear DCEUS intensity on the contrast side of the RMSM. The lognormal models were constructed using clinically derived (see section II.B) quantification parameters (normal liver and liver lesions) for the RT, MTT, and PI.

Multiplicative noise was applied to the DCEUS side of the simulation in order to compare errors caused by respiratory motion to those produced by noise. The gamma distribution multiplicative noise model proposed by Barrois et al[27] was used according to (4),

$$gamma(x;\kappa,\alpha) = \frac{x^{\kappa-1}e^{-\frac{x}{\alpha}}}{\Gamma(\kappa)\alpha^{\kappa}}, \tag{4}$$

where κ=3 and α=0.5. The k value of 3 was based on measurements performed by Barrois et al whereas the alpha value of 0.5 was derived based on the condition that the mode of the distribution (*Mo*) must have a value of 1. In order to apply the multiplicative noise from the gamma distribution each DCEUS frame of the simulation was multiplied by a random sample of a 300 x 300 matrix derived from the a gamma distribution with κ=3 and α=0.5. The random sample was generated using the "gamrnd" function part of MATLAB's Statistics Toolbox.

Three sets of simulations were run to study the effect of lesion size, in-plane and out-of-plane respiration amplitude. An additional set of simulations was run this time with multiplicative noise applied on the contrast side of the acquisition to investigate the effect of noise on the DCEUS quantification parameters extracted from the RMSM. The effect of lesion size on the DCEUS quantification parameters was studied with a set of simulations with increasing lesion radius between 10 and 35 px; the IPA was varied between 0 to 36 px and the OPA was set to 0 px. A set of simulations with a constant *OPA* of 10 px and a varying *IPA* between 0 to 36 px, a set with a constant *IPA* of 10px and a varying *OPA* between 0 to 36 px in order to evaluate the error introduced on the DCEUS quantification parameters from both in-plane and out-of-plane motion. The maximum amplitude of 36 px was chosen in order to simulate the clinical scenario in which the lesion is not visible in the imaging plane at the end phases of respiration. A set of simulations were also run with a constant *OPA* of 10 px and a varying *IPA* between 0 to 36 px with the presence of multiplicative noise on the DCEUS side of the acquisition.

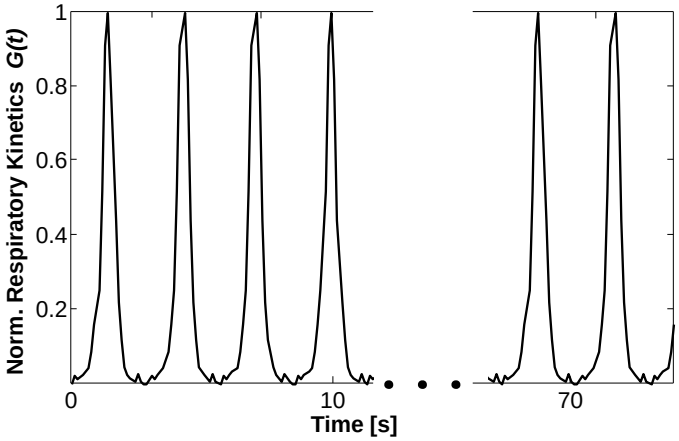

Fig. 3. Normalized respiratory kinetics curve extracted from patient data that was used to drive the respiration motion of the respiratory motion simulation model.

The mean linear intensity within a ROI corresponding to the initial position of the lesion on the contrast side of the RMSM (Fig. 4a) at time zero was extracted across time. Due to the

This article has been accepted for publication in a future issue of this journal, but has not been fully edited. Content may change prior to final publication. Citation information: DOI 10.1109/TMI.2015.2487866, IEEE Transactions on Medical Imaging

respiratory motion present in the simulation the lesion time intensity curve extracted will exhibit similar breathing artefacts as in the clinic. The lognormal indicator dilution model was fitted onto lesion time intensity curves extracted with and without the use of ARG. The quantification parameters of RT, MTT, area under the curve (AUC) and PI were calculated and compared to the input perfusion parameters of the RMSM. By comparing the error introduced on the quantification parameters the accuracy of DCEUS quantification with and without ARG can be assessed.

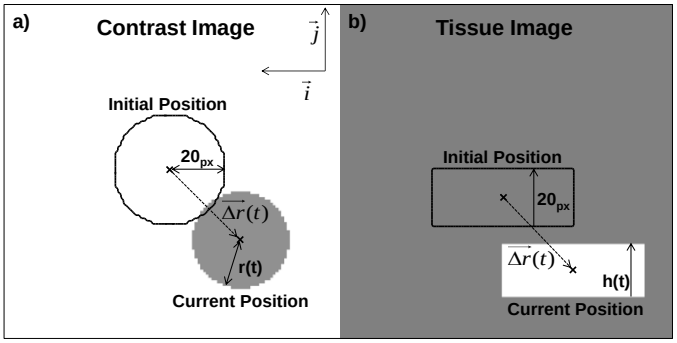

Fig. 4. Zoom-in on a simulated dual contrast imaging acquisition at the time of peak of the parenchyma (29 seconds). a) Simulated DCEUS side of the acquisition with the initial position of the lesion indicated (solid black circle) encompassing mostly the parenchyma with the lesion moved out of position in-plane by a vector $\Delta r(t)$ and a reduction of its radius from the initial radius of R_L (20 px) to $r(t)$ due to out-of-plane respiratory motion. b) Simulated tissue side of the acquisition with the moving structure out of position in-plane by a vector $\Delta r(t)$ and a variation in its height from h_0 (20 px) to $h(t)$ accounting for out-of-plane motion.

B. Clinical DCEUS Acquisitions

Twenty-two (22) patients (10 female, 12 male) with liver metastasis were imaged. The median age of the female patients was 69 (range, 47-72) and the male median age was 74 (range, 59-77). Approval for the scanning was obtained by the ethics review board of our hospital. Also the procedure was fully explained to all participating patients and informed consent was obtained.

The Philips iU22 scanner (Philips Medical Systems, Bothell, WA) along with the C5-1 curve-linear array probe was utilized for all imaging. The imaging frequency was set at 1.7 MHz and the pulsing scheme used was power modulation with a mechanical index (MI) of 0.06. One minute loops were acquired at a frame rate between 7-10 Hz in dual contrast imaging acquisition mode with an image resolution of 0.39mm/px. The time-gain-compensation (TGC) was set so that a very low level of uniform noise was present on the image before the arrival of the microbubbles, ensuring that the TGC was at the threshold of detection. In an effort to maintain a uniform pressure field the focus was set below the depth of the lesion. The Sonovue (Bracco s.p.a., Milan, Italy) microbubble contrast agent was injected as a 2.4mL bolus. The clinician maintained a constant imaging plane by monitoring the "tissue" side of the acquisition.

C. Image Data Analysis

The patient DICOM files were extracted from the Philips iU22 scanner and transferred to the commercial quantification software QLAB version 8.1 (Philips Medical Systems, Bothell, WA) for analysis. Both the arterial and late portal phases of the DCEUS loop were used to accurately draw a ROI encompassing the liver lesion. The frame at which the lesion was delineated was the reference that defined the breathing cycle phase to be extracted by the ARG algorithm. In particular this frame served as the "trigger" frame by which ARG was performed (see section II.D). The lesion time intensity curves from linearized image data were extracted from QLAB and were analyzed with and without the implementation of the ARG.

Non-linear regression fits of the lognormal indicator dilution model [26] were performed on the lesion time intensity curves using MATLAB's Curve Fitting Toolbox trust region algorithm. The quantification parameters of AUC, PI, RT, and MTT were extracted from the lognormal model fit. In addition the quality of fit of the lognormal model on to the data was assessed by calculating the coefficient of determination (R^2_{LN}). The quality of fit has been used in the literature[21], [23], [25] as a metric of the improvement in the reliability of DCEUS quantification.

The effect of respiration on the DCEUS acquisitions was quantified by calculating the respiration amplitude (*RA*) of the time intensity curves extracted without the use of ARG. The *RA* was calculated by first computing the frequency spectrum of the lesion time intensity curves. The faster varying respiration component of the lesion time intensity curve was between the respiration range of 0.1-0.5 Hz [28] in contrast to the slower changing lesion perfusion pattern that was below 0.1Hz (Fig. 5). The RA was calculated as the ratio between the area under the frequency spectrum between 0.1-0.5Hz and the area between 0-0.1Hz.

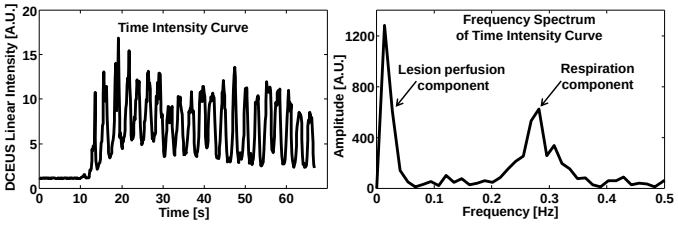

Fig. 5. Example of a clinical lesion time intensity curve extracted from a DCEUS acquisition under the influence of respiratory motion (left) and its frequency spectrum (right). The separation of the lesion perfusion and respiration components is clearly shown in the frequency domain.

D. ARG Algorithm

The ARG algorithm was applied on the tissue side of the dual contrast imaging acquisition. The MATLAB® (2012b, The MathWorks Inc., Natick, MA) scientific computing software was used to implement the ARG algorithm (Fig. 6).

The location and intensity of motion produced by bright structures in the loop was identified by subtracting each frame from the average from all the frames[29] and summing the result. Bright moving structures were identified on the trigger frame and the intensity of the motion corresponding to each structure was calculated as the average motion intensity encompassed by the structure. In addition a frequency domain analysis was performed to calculate the respiratory contents associated with each moving structure. A ROI was constructed

This article has been accepted for publication in a future issue of this journal, but has not been fully edited. Content may change prior to final publication. Citation information: DOI 10.1109/TMI.2015.2487866, IEEE Transactions on Medical Imaging

from the structure with the highest contents of respiratory motion and applied on the tissue loop to extract the time intensity curve. The troughs and peaks of the time intensity curve correspond to the time instances at which the acquisition was out-of-phase and in-phase with the trigger frame respectively. By removing the frames that were below 40% from the peak intensity the respiratory motion in the loop was reduced. The threshold value of 40% was a compromise between preserving enough time intensity curve data to perform a reliable fit of the lognormal indicator dilution model, while at the same time reducing the amount of respiratory motion in the loop. A more detailed description of the implementation of the ARG algorithm can be found in the literature[25].

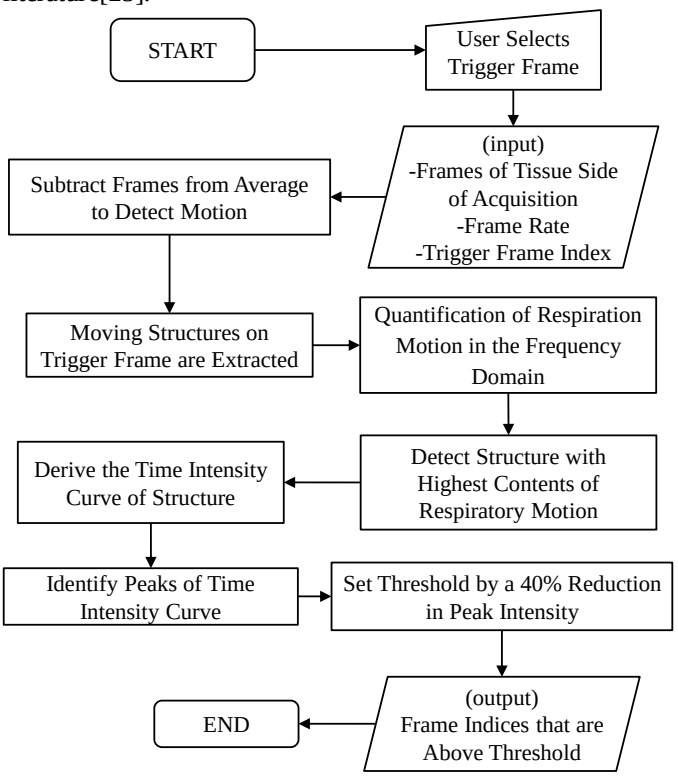

Fig. 6. Summary flowchart of the processes used to implement the ARG algorithm in MATLAB.

III. Results

From the simulations investigating the effect of lesion size with increasing IPA it was shown that as the lesion size decreases the percentage error in the parameters increases for the same IPA (Fig. 7). However when the IPA was normalized to the lesion radius of each simulation the percentage error of the quantification parameters was shown to be constant for the same IPA/R_L ratio (Fig. 8). The results reported hereafter are in reference to the IPA/R_L and OPA/R_L.

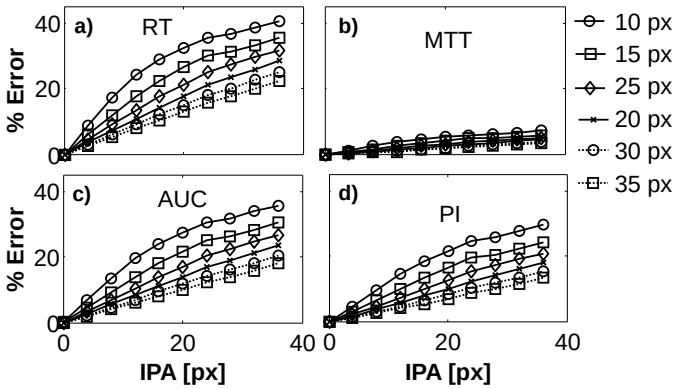

Fig. 7. RMSM results with increasing in-plane respiratory amplitude and different lesion sizes. The percentage error for a) RT, b) MTT, c) AUC, and d) PI is shown.

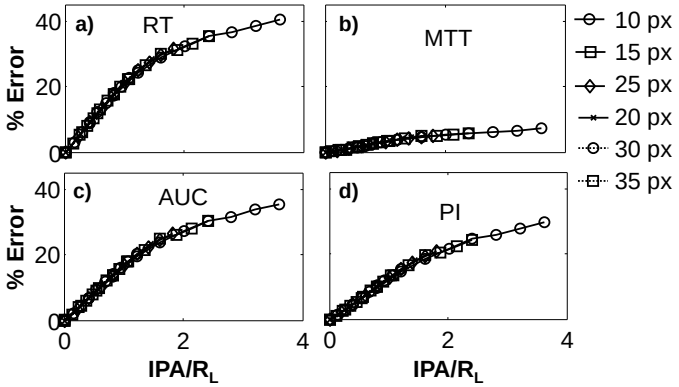

Fig. 8. RMSM results from Fig. 7 with the x-axis of the plots displaying the IPA normalized to the lesion radius (R_L=20px).

The results from the RMSM showed that ARG algorithm reduced the error in the quantification parameters introduced from in-plane respiratory motion (Fig. 9). The overall errors where reduced from a mean of 13.0% to a mean of 2.4%. Specifically for the RT the mean error was decreased from 20.0% to a mean of 3.9%, for the MTT from a mean of 3.1% to 1.3%, for the AUC from 16.4% to a mean of 2.6% and for the PI from a mean of 12.4% to 2.0%. In addition to reducing errors introduced from in-plane respiratory motion the ARG algorithm was shown to also reduce the errors from out-of-plane motion. The mean error introduced with increased OPA was reduced by 16.4%, 1.2%, 14.1% and 9.9% for the RT, MTT, AUC and PI respectively (Fig. 10).

The reduction in the mean percentage error of quantification parameters with the use of ARG was tested using the paired t-test at a significance level of 0.001. It was found to be statistically significant for the RT, AUC and PI ($p<0.001$) both for in-plane and out-of-plane respiratory motion. The reduction of the MTT percentage error was found not to be significant for the in-plane ($p=0.014$) and out-of-plane ($p=0.044$) motion. MTT did not suffer much from motion as it is a time parameter associated with the overall duration of the bolus that despite the respiratory noise it still remains unaffected. As an example, consider adding high frequency noise (respiratory noise) on a low frequency signal (MTT). The overall effective period of the low frequency signal remains unaffected.

This article has been accepted for publication in a future issue of this journal, but has not been fully edited. Content may change prior to final publication. Citation information: DOI 10.1109/TMI.2015.2487866, IEEE Transactions on Medical Imaging

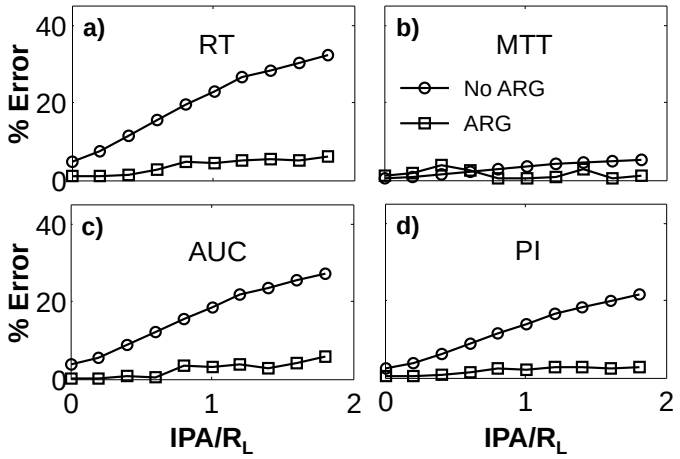

Fig. 9. Percent error of the quantification parameters with increasing in-plane respiratory amplitude with (squares) and without (circles) the use of the ARG algorithm.

The multiplicative noise introduced on the DCEUS simulation had no effect on the RT and MTT with the results with and without noise being almost identical [compare Fig. 9(a)-(b) with Fig. 11(a)-(b)]. However noise did increase the errors for the amplitude quantification parameters by a mean value of 50.0% for AUC and 50.0% for PI [compare Fig. 9(c)-(d) with Fig. 11(c)-(d)]. The error increase due to noise for the amplitude parameters was almost constant across increasing IPA with the calculated standard deviation of the mean increase in error being less than 0.6%.

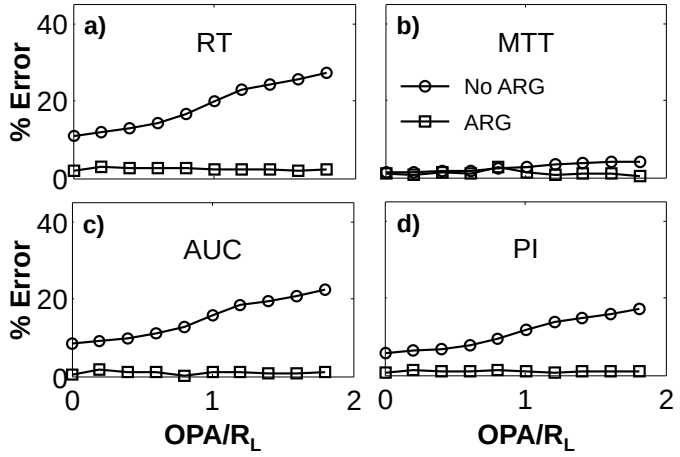

Fig. 10. Same as Fig.9 but with out-of-plane motion. Percent error of the quantification parameters with increasing out-of-plane respiratory amplitude with (squares) and without (circles) the use of the ARG algorithm.

The overall RMSM validity was evaluated by comparing the relationship between the R^2_{LN} and the respiration amplitude (*RA*) extracted both from the simulation and patient data. Simulation data using the parenchyma perfusion model extended to an *RA* of 1.1 whereas the clinical data extended to an *RA* of 2.2. This was attributed to the fact that clinical data include signal from nearby vessels, like veins, that can contribute to a higher linear intensity within the lesion ROI compared to the parenchyma. In order to investigate the effect of vessels to lesion DCEUS quantification parameters a set of simulations were run with constant OPA and variable IPA. The parenchyma perfusion model was replaced with a vein model with a RT of 27 seconds, a MTT of 54 seconds and a PI of 190 AIU derived from the clinical data. The results from both simulation sets were compared with the clinical data (Fig. 12). Both the clinical data and the simulations demonstrate a negative correlation with the R^2_{LN} decreasing as the *RA* increases without the use of ARG. The slope of the linear regression was -0.33 and -0.40 for the clinical and simulation data respectively. With the use of ARG the slope was decreased for both the patient (-0.12) and simulation data (-0.14).

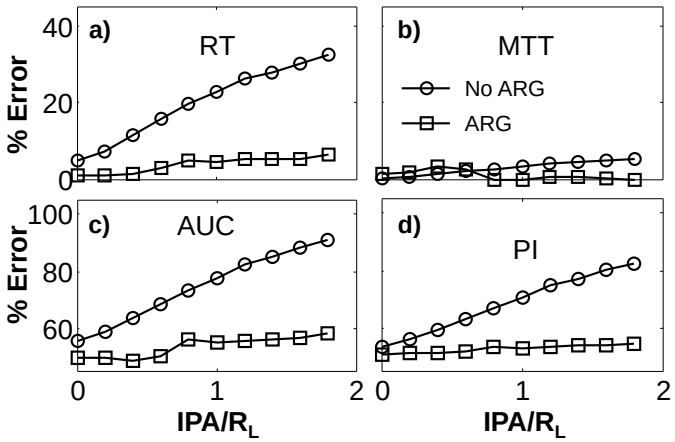

Fig. 11. Same as Fig. 9 but with added multiplicative noise. Percent error of the quantification parameters with the application of multiplicative noise under increasing in-plane respiratory amplitude with (squares) and without (circles) the use of the ARG algorithm.

IV. Discussion

In this study a RMSM was developed that was used to study the effectiveness of an ARG algorithm in increasing the absolute accuracy of liver lesion DCEUS quantification. The use of simulation to evaluate respiratory compensation algorithms for liver lesion DCEUS has been previously suggested by Renault et al[20]. The simulation by Renault et al examined the effects of respiration for a single in-plane and out-of-plane amplitude with only the contrast side of the acquisition being simulated. Furthermore the errors that respiration introduced on lesion time intensity curves were evaluated qualitatively without looking into specific quantification parameters. That study concluded that image registration based algorithms for respiratory motion compensation were inadequate in removing out-of-plane motion from liver DCEUS acquisitions. The independent component analysis (ICA) method proposed by Renault et al and the principal component analysis (PCA) examined by Mule et al[19] have been shown to remove both in-plane and out-of-plane motion from DCEUS loops. However only the end phases of the respiratory cycle can be extracted using ICA and PCA analysis, and since the acquisition is two dimensional there is the uncertainty whether a portion or any part of the lesion will be present on the extracted frames.

The RMSM used in this study considers a broad range of out-of-plane and in-plane respiratory motion amplitudes. The application of the ARG algorithm on the dual contrast imaging

This article has been accepted for publication in a future issue of this journal, but has not been fully edited. Content may change prior to final publication. Citation information: DOI 10.1109/TMI.2015.2487866, IEEE Transactions on Medical Imaging

mode simulation has been shown to significantly reduce the errors on DCEUS quantification parameters. Overall the implementation of the ARG algorithm significantly reduced the errors introduced by respiratory motion ($p<0.001$) from a maximum of 32.3% to less than 6.3%. ARG produced significant gains in DCEUS quantification parameter accuracy for the RT, AUC and PI ($p<0.001$) whereas the impact of ARG on MTT was not significant. This was also the case for a clinical study [24] where the MTT was found to be unaffected by the ARG algorithm.

The increase in the accuracy from the use of the ARG algorithm can improve clinical outcomes in liver DCEUS quantification. For example in a clinical study on liver lesion DCEUS quantification by Averkiou et al [10] the response of patients to treatment was detected as a mean change in the wash-in time ratio quantification parameter of 17% after the first treatment. Zocco et al [30] found significant changes from the baseline of -20% and -25% in the AUC and PI respectively for patients that had a response to hepatocellular carcinoma treatment. Both Averkiou et al and Zocco et al used respiratory gating to improve the accuracy of their quantitative analysis. These changes in the quantification parameters would be impossible to detect if there is an error of about 30% already present due to the respiratory motion. Furthermore in the quantification parameter reproducibility study performed by Averkiou et al an average deviation of 9% was calculated which is above the maximum residual error of 6.3% remaining after the use of ARG.

By taking into consideration multiplicative noise on the contrast side of the dual contrast imaging simulation no change was observed on the time quantification parameters of RT and MTT. The results were almost identical with the maximum difference being less than 1.8% for the RT and MTT extracted both with and without ARG. On the other hand the amplitude parameters of AUC and PI were severely affected with the value of the AUC error increasing by a maximum of 51.4% and of the PI by a maximum of 50.5%. Simulations run by Barrois et al [27] found absolute error differences for the AUC of 49.8-50.3% , the MTT of 15.5-22.0% and 4.3-5.6% for the RT. The simulations applied multiplicative noise directly onto each data point of the time intensity curve, corresponding to a mean signal from a 5x5 block of pixels, in contrast with the RMSM that takes the average within a 20px radius ROI. Thus the sample size used to calculate the values of the time intensity curve data points for the current study is 1257 compared with 25 from Barrois et al. The standard error of the mean, $SE = \frac{\sigma}{\sqrt{n}}$ [31], is thus expected to be higher for the smaller sample explaining the discrepancy between the results obtained from the two studies. Therefore the errors reported by Barrois et al are more relevant to parametric imaging studies rather than the modeling of the average perfusion of a liver lesion.

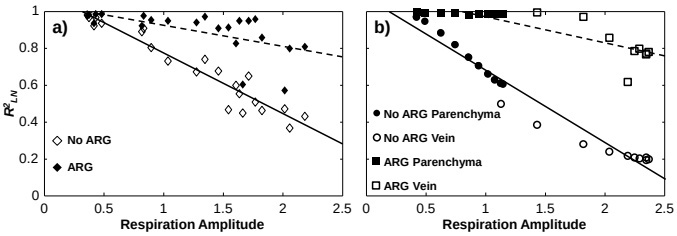

Fig. 12. Scatter plots of R^2_{LN} vs. respiration amplitude with and without the use of automatic respiratory gating (ARG) for a) clinical patient data and b) simulation results from the RMSM. The linear regression lines of the displayed data are also shown without (solid) and with (dotted) ARG.

The errors introduced from the gamma distribution noise model on the amplitude parameters can be predicted analytically. The mean and standard deviation can be calculated from the moments of the gamma distribution[32] and are given by $\mu = \kappa \times \alpha$ and $\sigma = \sqrt{k} \times \alpha$. Also by differentiating (4) the mode (i.e. maximum of the probability density function) can be calculated as $Mo = (\kappa - 1) \times \alpha$. By eliminating κ and α the mode can be written in respect to μ and σ as $Mo = \frac{\mu^2 - \sigma^2}{\mu}$. The multiplicative model used from the work of Barrois et al[27] uses the relationship between the standard deviation (σ), the mean (μ), and the shape parameter κ of the gamma distribution to estimate κ from DCEUS measurements of the standard deviation and mean linear intensity with increasing concentration of microbubbles. Since the relationship used [27] between σ and μ is a linear model $\sigma = slope \times \mu$ and also $\sigma = \frac{\mu}{\sqrt{\kappa}}$, derived from the moments of the gamma distribution, the mean, and the mode can directly related to the shape parameter κ by $\mu = \left(\frac{\kappa}{\kappa - 1} \right) \times Mo$. Consequently the mean (μ) linear intensity within the ROI will be one and a half times the value of the mean liner intensity before the gamma distribution noise was applied with parameters κ=3 and *Mo*=1 used in the RMSM. The overall mean error between the amplitude parameters extracted with and without multiplicative from the simulation was found to be 50.0% with a standard deviation of less than 0.5% verifying the analysis made. As already mentioned in the previous paragraph the error obtained from the simulations by Barrois et al for the AUC was between 49.8-50.3% agreeing with the prediction of the analysis presented.

Limitations of the RMSM include simplifications made compared to the complexity of clinical dual contrast imaging acquisitions. The shape of clinical lesions does not follow a strict spherical shape as used in the RMSM although an ellipsoidal shape is generally assumed for demonstration purposes[7]. In addition respiratory motion does not only cause rigid in-plane and out-of-plane motion but also results in deformation due to the elasticity of tissue. The deformation of the lesions due to respiratory motion was not accounted for in the RMSM. Despite of these limitations of the RMSM it offers

a controlled platform by which to study the absolute errors introduced by respiratory motion on DCEUs quantification parameters. Furthermore the RMSM has the potential to be used in the training of clinicians in DCEUS quantification in an effort to increase intra-observer and inter-observer agreement. This could be especially useful for multi-centre studies since the training can be performed remotely and data analysis can be centralized. Future studies of respiratory motion could also simulate 3D DCEUS acquisitions to investigate the effect of respiratory motion compensation schemes on DCEUS quantification. However 3D DCEUS is not currently used routinely in the clinic[33] thus there are not enough clinical data available to construct such a model.

Both the perfusion and respiration kinetics of the RMSM were derived from clinical dual contrast imaging acquisitions in an effort to maximize the clinical relevance of the model. The similarities of the relationship between R^2_{LN} and *RA* for the RMSM and the clinical data give confidence to the clinical suitability of the model (Fig. 12). This further reinforces that the results obtained for the error reduction in DCEUS quantification parameters are expected to occur in the clinic.

V. Conclusion

A RMSM was presented that takes into account in-plane, out-of-plane respiratory motion, and multiplicative noise. The RMSM was used to investigate the effectiveness of an ARG algorithm in increasing the accuracy of liver lesion DCEUS quantification by removing in-plane and out-of-plane motion from dual contrast imaging mode acquisitions. The use of RMSM clearly revealed that the ARG algorithm significantly reduces errors introduced from in-plane and out-of-plane respiratory motion. The time quantification parameters of RT and MTT remained almost unaffected under the presence of multiplicative speckle noise whereas the amplitude quantification parameters of AUC and PI showed a constant error of 50% from their set values. The relationship between the quality-of-fit (R^2_{LN}) and the respiration amplitude (*RA*) for both clinical and RMSM-simulated data was similar thus confirming the clinical relevance of the simulation. Finally, the RMSM has proven to be a useful tool in studying bolus kinetics and investigating the impact of ARG on the accuracy of liver lesion DCEUS quantification parameters.

References

[1] P. N. Burns, "Harmonic imaging with ultrasound contrast agents.," *Clin Radiol*, vol. 51 Suppl 1, pp. 50–5, Feb. 1996.

[2] C. Huang-Wei, A. Bleuzen, P. Bourlier, J. Roumy, A. Bouakaz, L. Pourcelot, and F. Tranquart, "Differential diagnosis of focal nodular hyperplasia with quantitative parametric analysis in contrast-enhanced sonography.," *Invest Radiol*, vol. 41, no. 3, pp. 363–8, Mar. 2006.

[3] L. Galiuto, B. Garramone, A. Scarà, A. G. Rebuzzi, F. Crea, G. La Torre, S. Funaro, M. Madonna, F. Fedele, and L. Agati, "The Extent of Microvascular Damage During Myocardial Contrast Echocardiography Is Superior to Other Known Indexes of Post-Infarct Reperfusion in Predicting Left Ventricular Remodeling," *J Am Coll Cardiol*, vol. 51, no. 5, pp. 552–9, Feb. 2008.

[4] R. Senior, M. Monaghan, M. L. Main, J. L. Zamorano, K. Tiemann, L. Agati, N. J. Weissman, A. L. Klein, T. H. Marwick, M. Ahmad, A. N. DeMaria, M. Zabalgoitia, H. Becher, S. Kaul, J. E. Udelson, F. J. Wackers, R. C. Walovitch, and M. H. Picard, "Detection of coronary artery disease with perfusion stress echocardiography using a novel ultrasound imaging agent: two Phase 3 international trials in comparison with radionuclide perfusion imaging.," *Eur J Echocardiogr*, vol. 10, no. 1, pp. 26–35, Jan. 2009.

[5] K. Wei, A. R. Jayaweera, S. Firoozan, A. Linka, D. M. Skyba, and S. Kaul, "Basis for detection of stenosis using venous administration of microbubbles during myocardial contrast echocardiography: bolus or continuous infusion?," *J Am Coll Cardiol*, vol. 32, no. 1, pp. 252–260, Jul. 1998.

[6] M. Averkiou, M. Bruce, S. Jensen, P. Rafter, T. Brock-Fishe, and J. Powers, "Pulsing schemes for the detection of nonlinear echoes from contrast microbubbles," in *9th European Symposium on Ultrasound Contrast Imaging*, 2004, pp. 17–24.

[7] S. R. Wilson and P. N. Burns, "Microbubble-enhanced US in body imaging: what role?," *Radiology*, vol. 257, pp. 24–39, 2010.

[8] A. Muhi, T. Ichikawa, U. Motosugi, H. Sou, H. Nakajima, K. Sano, M. Sano, S. Kato, T. Kitamura, Z. Fatima, K. Fukushima, H. Iino, Y. Mori, H. Fujii, and T. Araki, "Diagnosis of colorectal hepatic metastases: Comparison of contrast-enhanced CT, contrast-enhanced US, superparamagnetic iron oxide-enhanced MRI, and gadoxetic acid-enhanced MRI," *J. Magn. Reson. Imaging*, vol. 34, no. 2, pp. 326–335, Aug. 2011.

[9] F. Tranquart, A. Le Gouge, J. M. Correas, V. Ladam Marcus, P. Manzoni, V. Vilgrain, C. Aube, M. F. Bellin, L. Chami, M. Claudon, M. Cuilleron, J. Drouillard, B. Gallix, O. Lucidarme, D. Marion, A. Rode, J. P. Tasu, H. Trillaud, A. Fayault, E. Rusch, and B. Giraudeau, "Role of contrast-enhanced ultrasound in the blinded assessment of focal liver lesions in comparison with MDCT and CEMRI: Results from a multicentre clinical trial," *Eur. J. Cancer Suppl.*, vol. 6, no. 11, pp. 9–15, Sep. 2008.

[10] M. Averkiou, M. Lampaskis, K. Kyriakopoulou, D. Skarlos, G. Klouvas, C. Strouthos, and E. Leen, "Quantification of tumor microvascularity with respiratory gated contrast enhanced ultrasound for monitoring therapy.," *Ultrasound Med Biol*, vol. 36, no. 1, pp. 68–77, Jan. 2010.

[11] M. Bertolotto, G. Pozzato, L. S. Crocè, F. Nascimben, C. Gasparini, M. A. Cova, and C. Tiribelli, "Blood flow changes in hepatocellular carcinoma after the administration of thalidomide assessed by reperfusion kinetics during microbubble infusion: preliminary results.," *Invest Radiol*, vol. 41, no. 1, pp. 15–21, Jan. 2006.

[12] N. Lassau, S. Koscielny, L. Chami, M. Chebil, B. Benatsou, A. Roche, M. Ducreux, D. Malka, and V. Boige, "Advanced hepatocellular carcinoma: early evaluation of response to bevacizumab therapy at dynamic contrast-enhanced US with quantification--preliminary results.," *Radiology*, vol. 258, no. 1, pp. 291–300, Jan. 2011.

[13] C. F. Dietrich, M. A. Averkiou, J.-M. Correas, N. Lassau, E. Leen, and F. Piscaglia, "An EFSUMB introduction into Dynamic Contrast-Enhanced Ultrasound (DCE-US) for quantification of tumour perfusion.," *Ultraschall Med*, vol. 33, no. 4, pp. 344–51, Aug. 2012.

[14] E. Leen, M. Averkiou, M. Arditi, P. Burns, D. Bokor, T. Gauthier, Y. Kono, and O. Lucidarme, "Dynamic contrast enhanced ultrasound assessment of the vascular effects of novel therapeutics in early stage trials.," *Eur Radiol*, vol. 22, no. 7, pp. 1442–50, Jul. 2012.

[15] A. Thapar, J. Shalhoub, M. Averkiou, C. Mannaris, A. H. Davies, and E. L. S. Leen, "Dose-dependent artifact in the far wall of the carotid artery at dynamic contrast-enhanced US.," *Radiology*, vol. 262, no. 2, pp. 672–9, Feb. 2012.

[16] M. Lampaskis and M. Averkiou, "Investigation of the relationship of nonlinear backscattered ultrasound intensity with microbubble concentration at low MI.," *Ultrasound Med Biol*, vol. 36, no. 2, pp. 306–12, Mar. 2010.

[17] D. Klein, M. Jenett, H.-J. Gassel, J. Sandstede, and D. Hahn, "Quantitative dynamic contrast-enhanced sonography of hepatic tumors.," *Eur. Radiol.*, vol. 14, no. 6, pp. 1082–91, Jun. 2004.

[18] H. S. Markus and M. J. Harrison, "Estimation of cerebrovascular reactivity using transcranial Doppler, including the use of breath-holding as the vasodilatory stimulus.," *Stroke*, vol. 23, no. 5, pp. 668–73, May 1992.

[19] S. Mulé, N. Kachenoura, O. Lucidarme, A. De Oliveira, C. Pellot-Barakat, A. Herment, and F. Frouin, "An automatic respiratory gating method for the improvement of microcirculation evaluation:

application to contrast-enhanced ultrasound studies of focal liver lesions.," *Phys Med Biol*, vol. 56, no. 16, pp. 5153–65, Aug. 2011.

[20] G. Renault, F. Tranquart, V. Perlbarg, A. Bleuzen, A. Herment, and F. Frouin, "A posteriori respiratory gating in contrast ultrasound for assessment of hepatic perfusion.," *Phys Med Biol*, vol. 50, no. 19, pp. 4465–80, Oct. 2005.

[21] N. Rognin, R. Campos, J. Thiran, T. Messager, P. Broillet, P. Frinking, M. Mercier, and M. Arditi, "A new approach for automatic motion compensation for improved estimation of perfusion quantification parameters in ultrasound imaging," in *Proceedings of the 8th French Conference on Acoustics*, 2006, pp. 61–65.

[22] N. G. Rognin, M. Arditi, L. Mercier, P. J. A. Frinking, M. Schneider, G. Perrenoud, A. Anaye, J.-Y. Meuwly, and F. Tranquart, "Parametric imaging for characterizing focal liver lesions in contrast-enhanced ultrasound.," *IEEE Trans Ultrason Ferroelectr Freq Control*, vol. 57, no. 11, pp. 2503–11, Nov. 2010.

[23] J. Zhang, M. Ding, F. Meng, M. Yuchi, and X. Zhang, "Respiratory motion correction in free-breathing ultrasound image sequence for quantification of hepatic perfusion," *Med Phys*, vol. 38, no. 8, pp. 4737–4748, Aug. 2011.

[24] D. Christofides, E. L. S. Leen, and M. A. Averkiou, "Improvement of the accuracy of liver lesion DCEUS quantification with the use of automatic respiratory gating.," *Eur. Radiol.*, Apr. 2015. [Epub ahead of print]

[25] D. Christofides, E. Leen, and M. Averkiou, "Automatic respiratory gating for contrast ultrasound evaluation of liver lesions.," *IEEE Trans. Ultrason. Ferroelectr. Freq. Control*, vol. 61, no. 1, pp. 25–32, Jan. 2014.

[26] C. Strouthos, M. Lampaskis, V. Sboros, A. McNeilly, and M. Averkiou, "Indicator dilution models for the quantification of microvascular blood flow with bolus administration of ultrasound contrast agents.," *IEEE Trans Ultrason Ferroelectr Freq Control*, vol. 57, no. 6, pp. 1296–310, Jun. 2010.

[27] G. Barrois, A. Coron, T. Payen, A. Dizeux, and L. Bridal, "A multiplicative model for improving microvascular flow estimation in dynamic contrast-enhanced ultrasound (DCE-US): theory and experimental validation.," *IEEE Trans. Ultrason. Ferroelectr. Freq. Control*, vol. 60, no. 11, pp. 2284–94, Nov. 2013.

[28] S. Fleming, M. Thompson, R. Stevens, C. Heneghan, A. Plüddemann, I. Maconochie, L. Tarassenko, and D. Mant, "Normal ranges of heart rate and respiratory rate in children from birth to 18 years of age: a systematic review of observational studies.," *Lancet*, vol. 377, no. 9770, pp. 1011–8, Mar. 2011.

[29] A. Jain, *Fundamentals of Digital Image Processing*. Englewood Cliffs, NJ: Prentice-Hall, 1989.

[30] M. A. Zocco, M. Garcovich, A. Lupascu, E. Di Stasio, D. Roccarina, B. E. Annicchiarico, L. Riccardi, M. E. Ainora, F. Ponziani, G. Caracciolo, G. L. Rapaccini, R. Landolfi, M. Siciliano, M. Pompili, and A. Gasbarrini, "Early prediction of response to sorafenib in patients with advanced hepatocellular carcinoma: The role of dynamic contrast enhanced ultrasound," *J. Hepatol.*, vol. 59, no. 5, pp. 1014–1021, 2013.

[31] D. G. Altman and J. M. Bland, "Standard deviations and standard errors.," *BMJ*, vol. 331, no. 7521, p. 903, Oct. 2005.

[32] R. Scheaffer, M. Mulekar, and J. McClave, *Probability and Statistics for Engineers*, 5th ed. Cengage Learning, 2010.

[33] J. M. Hudson, R. Williams, C. Tremblay-Darveau, P. S. Sheeran, L. Milot, G. A. Bjarnason, and P. N. Burns, "Dynamic contrast enhanced ultrasound for therapy monitoring.," *Eur. J. Radiol.*, 2015.